Bull. Mater. Sci., Vol. 38, No. 3, June 2015, pp. 805–809. © Indian Academy of Sciences.

The effects of Tb^{3+} doping concentration on luminescence properties and crystal structure of BaF_2 phosphor

ZHENXING DU, QUANSHENG LIU*, TIANJIANG HOU, YUE SONG, XIYAN ZHANG and YANYU CUI

Engineering Research Center of Optoelectronic Functional Materials of the Ministry of Education, Changchun University of Science and Technology, Changchun 130022, PR China

MS received 23 September 2014

Abstract. **This paper is aimed at explaining the effects of Tb^{3+} concentration on structure and luminescence properties and clarifying the concentration quenching mechanism of Tb^{3+}. The lattice of BaF_2 decreases with the increase of Tb^{3+} ions concentration. The emission spectrum of BaF_2:Tb^{3+} consists of blue emission band and green emission band and corresponds to the transition of $^5D_3 \rightarrow {}^7F_J$ ($J = 0, 1, 2, 4, 5, 6$) and $^5D_4 \rightarrow {}^7F_J$ ($J = 2, 3, 4, 5, 6$) of Tb^{3+}. The optimum concentration of Tb^{3+} is 4 mol%, and the concentration quenching mechanism of Tb^{3+} can be interpreted by the dipole–quadrupole (d–q) interaction.**

Keywords. **BaF_2 phosphor; crystal structure; luminescence properties; X-ray diffraction; concentration quenching.**

1. Introduction

Nowadays, the development of high-energy physics, electromagnetic calorimeter and new nuclear medicine increasingly need the scintillators which possess the property of fast afterglow. In the field of high-energy physics, especially, we need the scintillators with high-density, high-efficiency and short decay time. The light energy can be easily absorbed, stored, transferred and converted by fluoride because of their outstanding merits of strong ionic, broad band gap, low phonon energy and little electron cloud extension effect.[1] With more and more research developments, people have found many scintillators, such as $TiCl_2$:I,[2] tungstate[3–5] and $Bi_4Ge_3O_{12}$.[6] It is well known that the BaF_2 crystal has various outstanding properties and been widely used in luminescent materials. It has been intensively discussed in the field of experiment and application for its rapid light-emitting component of subnanosecond.[7] Tb^{3+} ion is a crucial rare earth ion, which provides a fascinating example in luminescence material.[8] In order to searching for new scintillator materials, Tb^{3+} has been experimentally studied in recent times as an activator ion in BaF_2 and other wide bandgap hosts.[9–14] In 1985, Van der Weg *et al* studied the effect of Tb^{3+} doping concentration on the luminescence behaviour.[15] In 1999, Kang *et al* reported that the particle size, shape, crystallinity, etc., significantly affect the luminescence properties of Tb^{3+} ion.[16] In 2014, the authors present *ab initio* theoretical study of the $4f^8$ and $4f^75d$ manifolds of Tb^{3+}-doped BaF_2 cubic sites, gives the calculated electronic structure and spectroscopic parameters.[12] On the basis of foregoing, we have firstly studied BaF_2:Tb^{3+} phosphors with various Tb^{3+} ion concentrations, for discussing the effects of Tb^{3+} ion concentrations on the luminescence properties and crystal structure, explaining concentration quenching mechanism.

2. Experimental

2.1 *Samples preparation*

The synthesis of the BaF_2:Tb^{3+} phosphors were based on the high-temperature solid-state reaction method. The raw materials used in the preparation of the BaF_2:Tb^{3+} phosphors were BaF_2 (AR), Tb_4O_7 (99.99%) and Na_2SiF_6 as a charge compensation agent.[17–21] The raw materials were weighed by the stoichiometric amounts of BaF_2:xTb^{3+}, where x is Tb^{3+} ion concentrations varying from 0.01 to 0.12 and spacing 0.01. Then, the mixture raw materials were mixed sufficiently in the agate mortar for 30 min and put into alumina crucibles. Finally, phosphor samples with various Tb^{3+} ion concentrations were obtained through calcinations successively at 725°C for 2 h under a reducing atmosphere created by burning activated carbon.

2.2 *Characterization*

The crystal structure and phase composition of samples were characterized by the Japanese Rigaku Ultima IV powder X-ray diffraction (XRD) (CuKα 40 kV, 20 mA, $\lambda = 1.5406$ Å). The photoluminescence emission and excitation spectra were measured by a RF-5301 spectrophotometer equipped with a 150 W Xe lamp which is made by Japan Shimadzu Corporation. All the luminescence properties of the phosphor were studied at room temperature.

*Author for correspondence (liuqs@cust.edu.cn)

3. Results and discussion

3.1 *The structure of BaF_2:Tb^{3+} phosphor*

Figure 1 shows the XRD patterns of BaF_2:Tb^{3+} phosphors doping Tb^{3+} with different concentrations. The concentration successively are 1, 2, 3, 4, 5, 6, 7, 8, 9, 10, 11 and 12 at%. The diffraction patterns of BaF_2:Tb^{3+} with different concentrations identify with PDF card (no. 04-0452), indicating that the crystal structure is a face-centred cubic system with space group Fm−3n and the lattice parameters are $a = b = c = 0.62001$ nm. No second phases are observed, which indicate the phosphor is a single phase and the doped Tb^{3+} ions are incorporated into the matrix lattice. The diffraction peaks slightly shift right, indicating that the lattice parameters decrease. The reason might be that Tb^{3+} ion has a smaller radius than Ba^{2+} ion (0.923 nm for Tb^{3+} ion *vs.* 1.35 nm for Ba^{2+}), and the cubic lattice parameters of Tb^{3+}-doped BaF_2 shrinks slightly in comparison with that of pure BaF_2 sample.[22,23] The lattice parameters and unit cell volume are decreasing while Tb^{3+} taking place of Ba^{2+}. The lattice parameter of samples with doped Tb^{3+} ions concentration from 1 to 12 at% is 0.61858, 0.61721, 0.61689, 0.61622, 0.61598, 0.61593, 0.61515, 0.61491, 0.61472, 0.61395, 0.61361 and 0.61213 nm, respectively. Figure 2 is the crystal structure pictures of BaF_2, figure 2a is the atomic arrangement diagram and 2b is the anion coordination polyhedron of a cation around. Seeing from figure 2a, a Ba^{2+} ion is enclosed by eight F^- ions, so we think the coordination number should be 8. According to figure 2b, the coordination polyhedron of F^- ion is a regular hexahedron, a cation ion should lie in the centre of regular hexahedron.

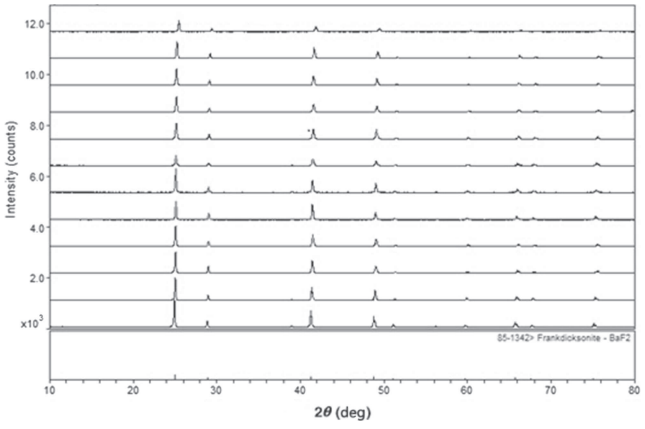

Figure 1. X-ray diffraction patterns of the samples.

3.2 *The luminescence properties of the samples*

Figure 3 shows the excitation and emission spectra of sample with 4 at% Tb^{3+} concentration, which excitation wavelength is 368 nm and monitor wavelength is 543 nm. As the excitation spectrum shown, there are six excitation peaks in the sample, peaking at 262, 284, 317, 350, 368 and 375 nm.[24] Therein, two main excitation peaks are at 368 and 375 nm. The broad excitation band less than 275 nm and peaking at about 262 nm caused by the spin-allowed 4f–5d transition of Tb^{3+} ion, and a series of absorption lines from 300 to 400 nm are attributed to the forbidden f–f transition of Tb^{3+} ion.[25] The emission spectrum consists of two sets of lines, the blue emission lines at shorter wavelengths, and weaker green emission lines at longer wavelengths. The arrows show positions of emission lines calculated from theoretical energies obtained earlier.[9,10] The ground term of the Tb^{3+} ion is $4f^8\ {}^7F$ and first excited term is $4f^8\ {}^5D$. Both terms are split by spin–orbit coupling and the transitions from the $^5D_4$ and $^5D_3$ multiplets to the different ^7F_J multiplets which result in the generation of green and blue emissions. The blue emissions of Tb^{3+} ion composed of six emission peaks, peaking at 492, 486, 470, 455, 438 and 418 nm are associated with the $^5D_3 \rightarrow {}^7F_J$ ($J = 0, 1, 2, 4, 5, 6$) transition. On the other hand, the green emissions consist of five emission peaks, peaking at 642, 617, 582, 543 and 492 nm because of the $^5D_4 \rightarrow {}^7F_J$ ($J = 2, 3, 4, 5, 6$) transition. Such an emission is dominated by the green band centred at 543 nm and associated with the $^5D_4 \rightarrow {}^7F_5$ transition, followed by the blue band centred at 492 nm associated with $^5D_4 \rightarrow {}^7F_6$, the red band centred at 582 nm associated with $^5D_4 \rightarrow {}^7F_4$ and the weaker red band centred at 617 and 642 nm

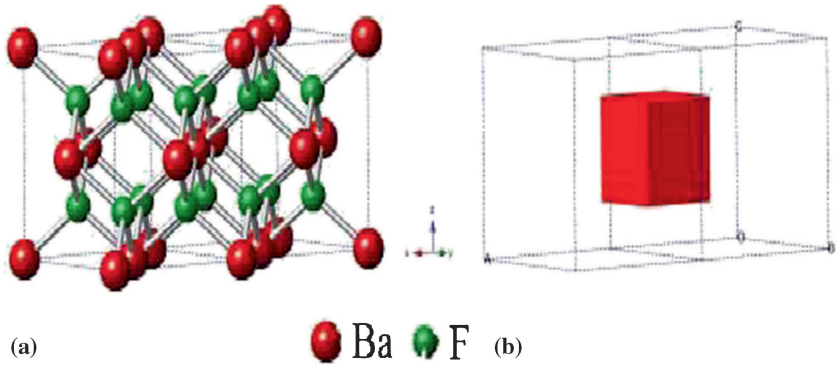

Figure 2. Crystal structure of BaF_2: (**a**) atomic arrangement diagram and (**b**) coordination polyhedron.

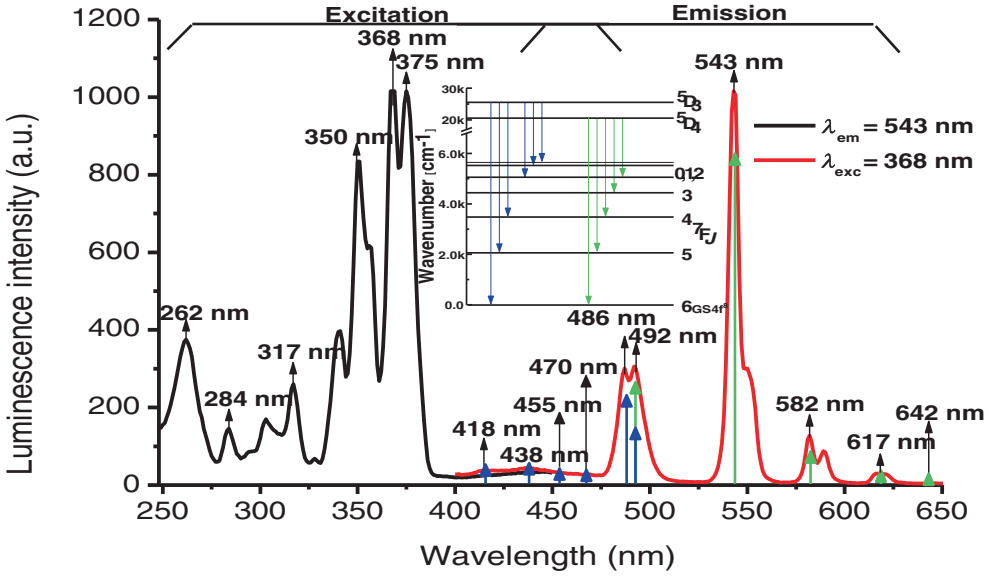

Figure 3. Room-temperature excitation (λ_{em} = 543 nm) and emission (λ_{exc} = 368 nm) spectra of BaF_2:Tb^{3+} (4 at%). The inset displays energy level of Tb^{3+}.

associated with $^5D_4 \rightarrow {}^7F_3$ and $^5D_4 \rightarrow {}^7F_2$.[11,12] In the chart inset in figure 2, we show the schematic energy level diagram of Tb^{3+} in BaF_2 based on experimental results presented in this paper.

3.3 *The effects of Tb^{3+} ion concentrations on luminescence properties*

The room-temperature excitation (monitored at 543 nm) and emission spectra (excited at 368 nm) of BaF_2:Tb^{3+} phosphors with starting composition of BaF_2:$x$$Tb^{3+}$ (x = 1, 2, 3, 4, 5, 6, 7, 8, 9, 10, 11, 12 at%) are shown in figures 4 and 5. As shown in the figures, the same change rule can be found in the excitation and emission spectra. When the Tb^{3+} ions concentration is less than 4 at%, the more the Tb^{3+} ions concentration is, the higher the luminescent intensity is. When Tb^{3+} ions are little, the number of luminescence centres is not enough. Therefore, the luminescent intensity is relatively low. With the increase of Tb^{3+} ions concentration, the quantities of luminescence centres increase and the luminescent intensity enlarge. When the concentration of Tb^{3+} ions is 4 at%, the intensities of excitation and emission reach maximum. Then, if the concentration of Tb^{3+} increases continually, the interaction of Tb^{3+}–Tb^{3+} increases, which leads to concentration quenching, so the emission intensity becomes lower, the more the Tb^{3+} ions concentration is, the lower the luminescent intensity is. Hence, it can be seen that the highest excitation and emission peaks were both obtained for 4 at% of Tb^{3+}.

In order to explain the concentration quenching mechanism, we take the emission band centred at 543 nm for example. The relationship between emission intensity and doped concentration of Tb^{3+} is shown in the inset of figure 4. According to above discussion, we think the original quenching concentration of Tb^{3+} in the BaF_2 host crystal is at 4 at%. The nonradiative energy transfer among luminescent centres can possibly occur due to exchange-type interactions, radiation reabsorption, or multipole–multipole interaction.[26] The exchange type is generally limited to interactions between RE ions in nearest neighbour or next nearest neighbour. Therefore, the fraction of RE ions in any event is little affected by exchange.[27] The very small overlapping of excitation and emission spectra in figure 2 implies that the radiation due to reabsorption cannot also be considered for nonradiative energy transfer among Tb^{3+} ions. Accordingly, electric multipole–multipole interactions should be predominantly considered for the energy transfer among Tb^{3+} ions, which are dependent on the distance among Tb^{3+} ions.

The interaction of Tb^{3+}–Tb^{3+} is dependent on the distance among Tb^{3+} ions. The critical distance among Tb^{3+} ions at the quenching concentration R_c can be estimated by the equation[27]

$$R_c \approx 2 \times (3V/4\pi x_c N)^{1/3}, \quad (1)$$

where V is the volume of the unit cell, x_c the quenching concentration of activator ion, and N the number of formula units per unit cell. According to the above discussion, $N = 4$, $x_c = 0.04$ and $V = 23.399$ nm^3; equation (1) yields $R_c \approx 1.409$ nm.

When electric multipolar interactions are involved in energy transfer, there are three possible types of interactions dipole–dipole, dipole–quadrupole and quadrupole–quadrupole. According to Dexter's theory,[28] if energy transfer occurs among activators of the same type, then the type of multipolar interactions can be identified by correlating activator's concentration (x) with emission intensity (I)[26,29]

$$I/x = K \times \left(1 + \beta \times x^{Q/3}\right)^{-1}, \quad (2)$$

where K and β are the constants for the same excitation condition for a given host crystal. The values of Q are

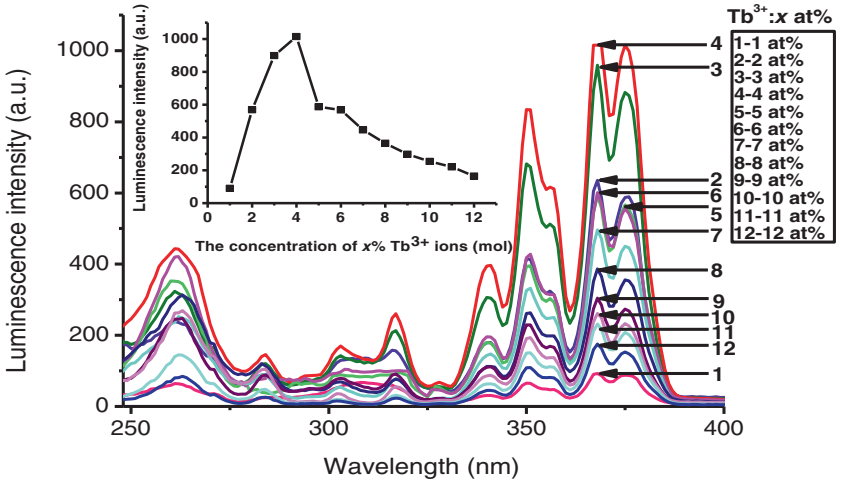

Figure 4. Excitation spectra of phosphors with various Tb^{3+} ion concentrations. The inset displays the relationship between luminescence intensity and concentration of Tb^{3+} ions.

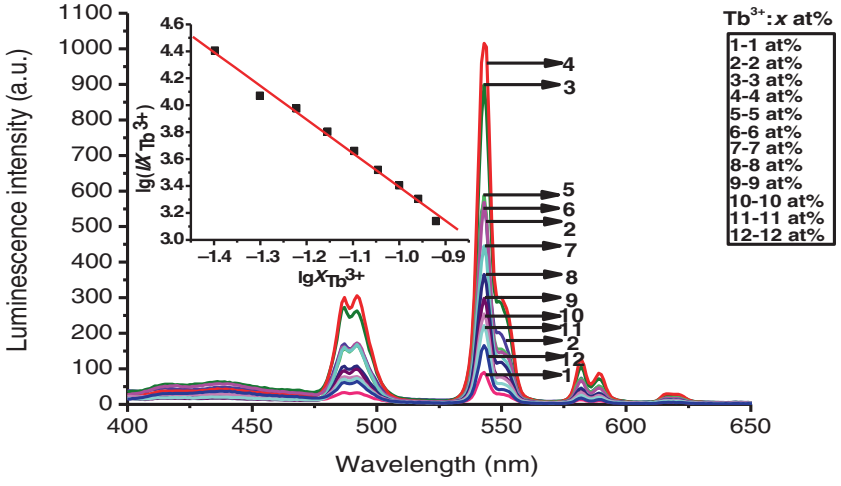

Figure 5. Emission spectrum of phosphors with various Tb^{3+} ion concentrations. The inset displays the plot of $\lg(I/x_{Tb^{3+}})$ *vs.* $\lg(x_{Tb^{3+}})$ in the selected Tb^{3+} phosphor.

six, eight and ten for dipole–dipole, dipole–quadrupole and quadrupole–quadrupole interactions, respectively.

To calculate the value of Q for the Tb^{3+} sites in BaF_2, the plot of $\lg(I/x_{Tb^{3+}})$ *vs.* $\lg(x_{Tb^{3+}})$ was attempted for $\lambda_{exc} = 368$ nm using the data in figure 5. The results are shown in the diagram as shown in the inset of figure 5. From the slope of the best fitted straight line is -2.503, the value of Q [via equation (2)] is calculated as 7.509. This value is fairly close to eight. Accordingly, it is suggested that the dominant multipolar interaction character of the Tb^{3+} emission is dipole–quadrupole coupling.

4. Conclusions

The luminescence properties, including excitation and emission spectra, concentration quenching of Tb^{3+}, and the structure of BaF_2:Tb^{3+} are systematically investigated. The crystal structure of BaF_2:Tb^{3+} phosphor was face-centred cubic structure. The BaF_2:Tb^{3+} phosphor has six excitation peaks, peaking at 262, 284, 317, 350, 368 and 375 nm. The emission spectrum of a Tb^{3+} ion composed of five bands associated with the $^5D_4 \rightarrow {}^7F_J$ ($J = 2$, 3, 4, 5, 6) transition. The major emission spectrum peak is at 543 nm corresponding to the $^5D_4 \rightarrow {}^7F_5$ transition of Tb^{3+}. The dominant multipolar interaction character of the Tb^{3+} emission is dipole–quadrupole coupling. The BaF_2:Tb^{3+} phosphors employ ascendant luminescence properties. It is indicated that the produced BaF_2:Tb^{3+} phosphors are promising materials for future consideration and experimentation in nuclear medicine or nuclear physics.

Acknowledgements

This work was supported by the projects of Jilin Science and Technology Bureau (no. 201201117 and no. 20090348), of Jilin Development and Reform Commission

(no. 2011FGW03) and of Changchun Science and Technology Bureau (no. 2013045).

References

1. Liang H B, Tian Z F and Zhong J P 2001 *Chin. J. Lumin.* **32** 411
2. Rosette K H, Farukhi M R, Kramer G R, Swinehart C and Hofstadter R 1970 *IEEE Trans. Nucl. Sci.* **17** 89
3. Mai M and Feldmann C 2012 *J. Mater. Sci.* **47** 1472
4. Rzhevskaya V, Spasskiĭ D A, Kolobanov V N, Mikhaĭlin V V, Nagornaya L L, Tupitsina I A and Zadneprovskiĭ B I 2008 *Opt. Spectrosc.* **104** 415
5. Nikl M, Bohacek P, Vedda A, Fasoli M, Pejchal J, Beitlerova A, Fraternali M and Livan M 2008 *J. Appl. Phys.* **104** 3514
6. Marinova V, Lin S H and Hsu K Y 2005 *J. Appl. Phys.* **98** 3527
7. Laval M, Moszyński M, Allemand R, Cormoreche E, Odru P and Vacher J 1983 *Nucl. Instr. Meth.* **206** 169
8. Blasse G and Grabmaier B C 1995 *Luminiscent materials* (Springer Verlag: Berlin)
9. Wojtowicz A J, Janus S and Piatkowski D 2009 *J. Lumin.* **129** 1594
10. Wojtowicz A J 2009 *Opt. Mater.* **31** 1772
11. Witkowski M E and Wojtowicz A J 2011 *Opt. Mater.* **33** 1535
12. Pascual J L, Barandiarán Z and Seijo L 2014 *J. Lumin.* **145** 808
13. van Pieterson L, Reid M F and Burdick G W 2002 *Phys. Rev. B* **65** 79
14. Zhang C M, Hou Z Y, Chai R T, Cheng Z Y, Xu Z H, Li C X, Huang L and Lin J 2010 *J. Phys. Chem. C* **114** 6928
15. Van der Weg W F, Popma T J A and Vink A T 1985 *J. Appl. Phys.* **57** 5450
16. Kang Y C, Lenggoro I W, Park S B and Okuyama K 1999 *J. Phys. Chem. Solids* **60** 1855
17. Quan Z W, Yang D M, Yang P P, Zhang X M, Lian H Z, Liu X M and Lin J 2008 *Inorg. Chem.* **47** 9509
18. Li W M and Leskela M 1996 *Mater. Lett.* **28** 491
19. Cao F B, Chen Y J, Tian Y W, Xiao L J and Li L K 2010 *Appl. Phys. B: Lasers Opt.* **98** 417
20. Li P, Wang Z, Yang Z, Guo Q and Fu G 2009 *Mater. Res. Bull.* **44** 2068
21. Radzhabov E and Kurobori T 2004 *J. Phys.: Condens. Matter* **16** 1871
22. Kingery W D, Bowen H K and Uhlmann D R 1976 *Introduction to ceramics* (Wiley: New York)
23. Jia G, Huang Y, Song Y, Yang M, Zhang L and You H 2009 *Eur. J. Inorg. Chem.* **2009** 3721
24. Raju K V, Raju C N, Sailaja S, Rambadu U and Reddy S 2012 *Ferroelectr. Lett.* **39** 117
25. Wei R F, Zhang H, Li F and Gao H 2012 *J. Am. Ceram. Soc.* **95** 34
26. Van Uitert L G 1967 *J. Electrochem. Soc.* **114** 1048
27. Jung K Y and Seo J H 2008 *Electrochem. Solid-State Lett.* **11** J64
28. Dexter D L 1953 *J. Chem. Phys.* **21** 836
29. Ozawa L and Jaffe P M 1971 *J. Electrochem. Soc.* **118** 1678